

Assessment of the Focal Hepatic Lesions Using Diffusion Tensor Magnetic Resonance Imaging

Siham Ait Oussous, Saïd Boujraf¹, Imane Kamaoui²

Department of Radiology and Clinical Imaging, University Hospital of Fez, ¹Department of Biophysics and Clinical MRI Methods, Faculty of Medicine and Pharmacy, University Hospital of Fez, Fez, ²Department of Radiology, University Hospital of Oujda, Morocco

Submission: 24-02-2016 Accepted: 06-04-2016

ABSTRACT

The goal is assessing the diffusion magnetic resonance imaging (dMRI) method efficiency in characterizing focal hepatic lesions (FHLs). About 28-FHL patients were studied in Radiology and Clinical Imaging Department of our University Hospital using 1.5 Tesla MRI system between January 2010 and June 2011. Patients underwent hepatic MRI consisting of dynamic T1- and T2-weighted imaging. The dMRI was performed with b-values of 200 s/mm² and 600 s/mm². About 42 lesions measuring more than 1 cm were studied including the variation of the signal according to the b-value and the apparent diffusion coefficient (ADC). The diagnostic imaging reference was based on standard MRI techniques data for typical lesions and on histology after surgical biopsy for atypical lesions. About 38 lesions were assessed including 13 benign lesions consisting of 1 focal nodular hyperplasia, 8 angiomas, and 4 cysts. About 25 malignant lesions included 11 hepatocellular carcinoma, 9 hepatic metastases, 1 cholangiocarcinoma, and 4 lymphomas. dMRI of soft lesions demonstrated higher ADC of 2.26 ± 0.75 mm²/s, whereas solid lesions showed lower ADC 1.19 ± 0.33 mm²/s with significant difference ($P = 0.05$). Discrete values collections were noticed. These results were correlated to standard MRI and histological findings. Sensitivity of 93% and specificity of 84% were found in diagnoses of malignant tumors with an ADC threshold of 1.6×10^{-3} mm²/s. dMRI is important characterization method of FHL. However, it should not be used as single criteria of hepatic lesions malignity. MRI, clinical, and biological data must be correlated. Significant difference was found between benign and solid malignant lesions without threshold ADC values. Hence, it is difficult to confirm ADC threshold differentiating the lesion classification.

Key words: Apparent diffusion coefficient, diffusion magnetic resonance imaging, focal hepatic lesion

INTRODUCTION

The diffusion magnetic resonance imaging (dMRI) constitutes a main imaging approach in the exploration of the focal hepatic pathologies because it offers a high resolution and contrast while it is completely noninvasive imaging approach allowing to produce information on the morphological and functional aspect of the human body.^[1-7]

The dMRI is based on the qualitative analysis of the signal intensity and the quantitative aspects based on the calculation of the apparent diffusion coefficient (ADC) in the investigated tissue. This technique uses an endogenous contrast mechanism that based on the self-diffusion of the tissue water and does not require any exogenous contrast agent. In addition, the dMRI is possible to be achieved in patients presenting contraindications for gadolinium contrast agents such as patients suffering from severe renal

deficiency, systematic nephrogenic fibrosis, and pregnant patients.^[1-9]

In clinical practice, the characterization of FHLs is an essential stage in the care of the patients. Hence, the diagnostic approach allowing the differentiation of benign and malignant lesions is also important for the histological classification of lesions types. Early clinical applications of the diffusion imaging in the liver demonstrated the sensitivity of this technique to hepatic lesions compared to standard MRI techniques such as T2-weighted MRI, especially in metastases.^[1-9]

This is an open access article distributed under the terms of the Creative Commons Attribution-NonCommercial-ShareAlike 3.0 License, which allows others to remix, tweak, and build upon the work non-commercially, as long as the author is credited and the new creations are licensed under the identical terms.

For reprints contact: reprints@medknow.com

Address for correspondence:

Dr. Saïd Boujraf, Department of Biophysics and Clinical MRI Methods, Faculty of Medicine and Pharmacy, University Hospital of Fez, BP 1893, Km 2.200, Sidi Hrazem Road, Fez 30000, Morocco.
E-mail: sboujraf@gmail.com

How to cite this article: Ait Oussous S, Boujraf S, Kamaoui I. Assessment of the Focal Hepatic Lesions Using Diffusion Tensor Magnetic Resonance Imaging. J Med Sign Sence 2016;6:99-105.

The goal of our work is to study of the dMRI in the assessment of the FHLs that is generally an important stage before achieving any invasive exploration or surgery.

This retrospective study suggests two targets; first, estimating the capability of the diffusion to characterize the FHLs by analyzing the signal variation according to b-values used and by measuring the average ADC within the hepatic lesions. Second, to estimate the relevance of the ADC threshold value of $1.6 \times 10^{-3} \text{ mm}^2/\text{s}$ in our MRI system. Indeed, this value is the threshold suggested by the literature to differentiate the benign and malignant lesions.

MATERIALS AND METHODS

Patients Selection

All patients' data were retrieved from the PACS imaging archive. Moreover, 50 patients were found with hepatic MRI; these patients were recorded in the MRI unit of the Department of Radiology and Clinical Imaging of our University Hospital, during the period between January 2011 and March 2012. All patients also underwent characterization of their hepatic lesions using other imaging modalities such as ultrasound and/or computed tomography (CT)-scan, and pretherapeutical assessments. Only the FHLs of more than 10 mm in diameter were retained. The most voluminous two lesions were included in the study for patients with multiple lesions.

The exclusion criteria were infracentimetric lesions, patients treated by chemotherapy and/or chemoembolization, radio-frequency therapy, and finally patients who underwent inappropriate MRI protocol and/or noninterpretable MRI data. Finally, only 28 patient's data were useful for this retrospective study.

The Imaging Protocol

All the patients underwent identical MRI protocol using 1.5 Tesla (General Electric). Finally, 28 patients were retained, with and hepatic MRI protocol consisting of fast spin echo (FSE) T2-weighting, T1-weighting, and dMRI with b-values of 200 and 600 s/mm^2 . Explorations with dynamic Liver Acquisition with Volume Acceleration (LAVA) in gradient-echo mode were achieved before and after injection of 0.2 mg/kg of gadolinium bolus.

The standard hepatic MRI protocol used in all patients, this included axial T1-weighting with double echo in phase and in phase opposition (with a repetition time/echo time of 145/49 ms for "in phase" and 145/2.3 ms "in phase opposition," flip angle of 80, matrix size 416×256 , slice thickness 4 mm, interslice gap of 0.5 mm, field of view $46 \text{ mm} \times 46 \text{ mm}$); the axial T2-weighting with single shot FSE (with repetition time/echo time 738/90 ms, matrix,

320×224 , slice thickness of 6 mm; interslice gap of 2 mm, field of view of $40 \text{ mm} \times 40 \text{ mm}$); the T2-weighting using Fast Imaging Employing Steady State Acquisition (with repetition time/echo time 3.8/1.7 ms, flip angle of 70, matrix size of 192×288 , slice thickness 4 mm, interslice gap of 2 mm, field of view $38 \text{ mm} \times 38 \text{ mm}$); the axial T2-weighting of FSE with fat suppression (with repetition time/echo time 2455/65 ms, flip angle of 19, matrix size 416×320 , slice thickness of 4 mm; interslice gap of 0.5 mm field of view $40 \text{ mm} \times 40 \text{ mm}$), with respiratory gating; finally, LAVA in gradient echo mode was used before and after injection of 0.2 mg/kg of gadolinium bolus (with repetition time/echo time of 3.3/1.5 ms, matrix size of 260×260 , the slice thickness of 3.8 mm; interslice gap of 1.9 mm, and an asymmetrical field of view of $46 \text{ mm} \times 41.4 \text{ mm}$).

Diffusion Magnetic Resonance Imaging Protocol

The axial dMRI was done using single-shot echo-planar imaging with respiratory gating and parallel imaging acquisition approach. The diffusion parameters were b-values of 200 and 600; the imaging parameters were repetition time/echo time of 5750/66.8 ms, the acquisition matrix size was 96×96 , the slice thickness was 7 mm; interslice gap was 0 mm, and the field of view was $40 \text{ mm} \times 40 \text{ mm}$. The dMRI protocol was achieved before injecting the contrast agents while the diffusion acquisition was lasting 50 s.

Magnetic Resonance Image Analysis

All MRIs were analyzed by two senior radiologists specialized in digestive imaging on the postprocessing consol. Both specialists assessed images with b-values of 200 and 600 s/mm^2 for various hepatic lesions.

Qualitative signal intensity in each hepatic lesion was evaluated and compared to the intensity in the neighboring adjacent hepatic parenchyma for the dMRIs with b-values of 200 and 600 s/mm^2 . The ADC maps were calculated using commercially available software. Region of interest (ROI) was established in each hepatic lesion ADC map and in the T2- and T1-weighted images obtained after contrast agent administration.

To ensure identical ROI was measured in all type of images in the same coordinates, an application was used for this purpose. This allowed measuring the ROI in all T1 and T2, diffusion images acquired with different b-values and ADC maps.

Our typical ROI was 100 mm^2 . The ADC was measured for the various lesions. Two measurements were achieved in each lesion and also within two healthy hepatic parenchyma tissues. The average value for each lesion and each healthy tissue was retained [Figure 1].

Final Diagnosis

The final diagnosis was based on MRI semiological and pathognomonic characteristics when they are yielding sufficient arguments. A histological confirmation was obtained in 8 patients including 6 biopsies and 2 surgeries. Other lesions diagnosis was also supported the biological assessment, the contribution of other imaging techniques such CT-scan and ultrasound, and arteriography performed before the chemoembolization of the hepatocellular carcinoma (HCC), and finally by the evolving follow-up.

Statistical Analysis

The ADC values were collected from 38 lesions in 28 patients. These values were compared to various types of focal lesions, and the analysis of variance was performed. Groups of benign and malignant lesions were compared using the Student's *t*-test. The average ADC results were expressed in ($\times 10^{-3}$ mm²/s \pm standard deviation). The $P < 0.05$ was considered to be the threshold of the significant statistical difference in all performed tests. The corresponding sensitivity and the specificity were measured.

RESULTS

Our population contained 15 males and 13 females with an average age of 58-year-old ranging from 24 to 72-year-old. The patients series contained 38 FHLs including 13 benign lesions of angiomas (n : 8), an FNH (n : 1), and cysts (n : 4) with one hydatid cyst; the 25 malignant lesions included HCC (n : 11), metastases (n : 9), lymphomas (n : 2), and cholangiocarcinoma (n : 1). All lesions measured more than 10 mm in diameter with an average size of 44 mm varying from 20 to 120 mm. The signal change analysis in dMRI according to the b-value demonstrated decreased signal

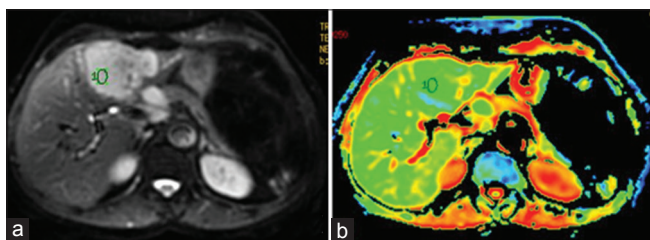


Figure 1: The diffusing weighted image with a b-value of 600 s/mm² (a) and the apparent diffusion coefficient map (b) are well demonstrating the hepatic lesion

in the cystic lesions with a b-value of 600, whereas other lesions did not demonstrate a significant signal change in lesion signal with higher b-value of 600.

The average ADC values in various types of lesions are reported in Table 1 and their visual comparison is reported in Figure 2. The average ADC value in the benign lesions was $2.09 \pm 0.75 \times 10^{-3}$ mm²/s, whereas the average ADC value in the malignant lesions lowered to $1.19 \pm 0.6 \times 10^{-3}$ mm²/s. Indeed, a significant difference was found in ADC between malignant and benign lesions [Figure 3] with a $P < 0.0001$ [Table 2].

dMRI demonstrated was sensitivity of 93% and specificity of 84% in the diagnosis of malignant lesions while a classification threshold of 1.6×10^{-3} mm²/s was used. A significant difference was found between ADCs measured in benign and malignant hepatic lesions with a $P = 0.0002$ [Figure 3]. The evaluation of dMRIs with a b-value of 600 s/mm² and the ADC maps were done by selecting a ROI within the lesion and in the right side which is free of lesion part of the hepatic parenchyma tissue presenting less vascular structure [Figures 4-6]. This allows avoiding the liver flow artifacts connected to vessels.

DISCUSSION

The dMRI has proven a great and growing interest of in hepatic pathology compared to other MRI techniques. Indeed, dMRI is a completely noninvasive technique

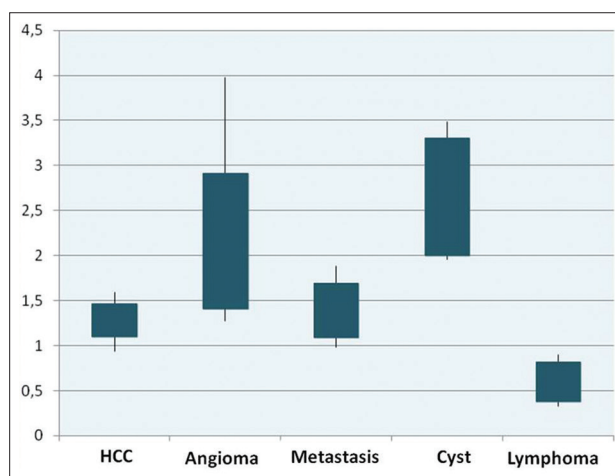


Figure 2: The apparent diffusion coefficient values (in $10^{-3} \times \text{mm}^2/\text{s}$) measured in the hepatic lesions

Table 1: Average apparent diffusion coefficient in the liver lesions obtained for a b-value of 600 s/mm² for different types of lesions of both categories of benign and malignant

	FNH (n=1)	ANG (n=8)	HCC (n=11)	META (n=9)	LYMP (n=4)	CYSTES (n=4)	CC (n=1)
Lesion ADC	1.52	2.16 \pm 0.75	1.4 \pm 0.18	1.39 \pm 0.30	0.6 \pm 0.22	2.61 \pm 0.69	1.15
Liver ADC	2.05	1.46 \pm 0.42	1.43 \pm 0.34	1.65 \pm 0.75	1.76 \pm 0.35	1.71 \pm 0.25	1.10

Results are expressed in $\times 10^{-3}$ mm²/s. FNH – Focal nodular hyperplasia; ANG – Angioma; HCC – Hepatocellular carcinoma; META – Hepatic metastasis; LYMP – Lymphoma; CC – Cholangiocarcinoma; ADC – Apparent diffusion coefficient

that does not require contrast agent administration that is acquired in very short time with possibility of better detection of the hepatic lesions with differentiating benign and malignant types and the quantification of the tissues alteration changes such the fibrosis that is not demonstrable in conventional MRI [Figure 7].

Hence, the diffusion weighted imaging and quantitative ADC measurements was proven to be efficient to characterize the FHLs and particularly differentiating the benign from malignant lesions.

The first study was achieved by Müller *et al.* in 1994 by, the ADC was measured within the hepatic focal lesions including three cysts, three hemangioma, and one metastatic HCC.^[10] These results showed elevated ADC values in the benign lesion including cysts and angiomas and lower ADC values in the malignant lesions such as metastases and HCC. Following studies have confirmed that average ADC in the benign lesions was significantly higher compared malignant lesions.^[11-13]

So far, the analysis of all published studies results do not allow to sort out a threshold value of ADC loosen (to kick away) a value of reliable and reproducible standardized ADC allowing to assess the benign and the malignant lesions, since all obtained ADC values are scattered, thus are not applicable in the clinical routine. These dispersed results are mainly due to the incoherence and heterogeneity of MRI and dMRI and also the nature of lesions included in the benign group of lesions. Mostly, the benign group of lesions

Table 2: Average apparent diffusion coefficient in the liver lesions obtained for a b-value of 600 s/mm² for both categories of benign and malignant lesions

	Benign lesions	Malignant lesions
Lesion ADC	2.09±0.75	1.19±0.6
Liver ADC	1.74±0.3	1.48±0.28

ADC – Apparent diffusion coefficient

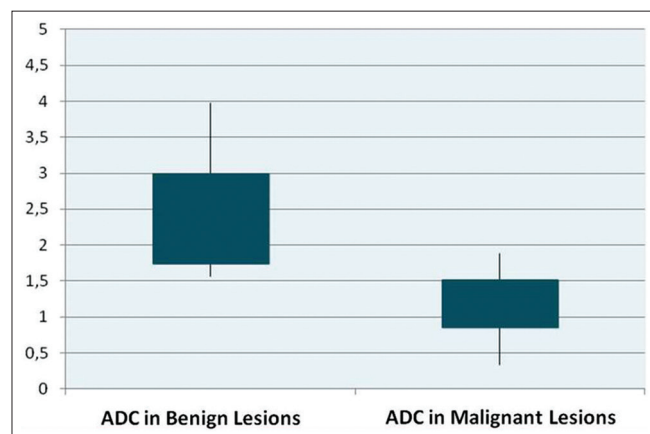


Figure 3: The apparent diffusion coefficient values (in $10^{-3} \times \text{mm}^2/\text{s}$) measured in the benign versus malignant lesions

is composed of cysts and angiomas and rarely FNH and adenomas [Figure 8]. Indeed, the cystic and angiomatous lesions have a very high average ADC values of $3.40 \times 10^{-3} \text{mm}^2/\text{s}$ and $2.26 \times 10^{-3} \text{mm}^2/\text{s}$, respectively; in fact, this selection of lesions contribute to significantly increase artificially the average ADC value when they are associated with benign lesions tissues. It is thus easier to highlight a significant difference of average ADC value of between benign and malignant tumors when cysts and angiomas are included in the group of benign tumors.

Despite reported constraint, threshold of ADC value was suggested to allow characterizing the hepatic lesions. Parikh *et al.* suggested a threshold ADC of $1.60 \times 10^{-3} \text{mm}^2/\text{s}$; hence, lower ADC was considered corresponding to malignant lesion.^[13] Gourtsoyianni *et al.* studied 37 lesions including 15 cysts, 7 angiomas, 13 metastases, and 2 HCC, they reported a threshold of ADC lower than $1.47 \times 10^{-3} \text{mm}^2/\text{s}$ for the malignant lesions diagnosis.^[14] Gourtsoyianni *et al.* demonstrated that the threshold ADC value in solid lesions is much lower ($1.04 \times 10^{-3} \text{mm}^2/\text{s}$) compared to earlier reported results.^[14] Recently, Miller

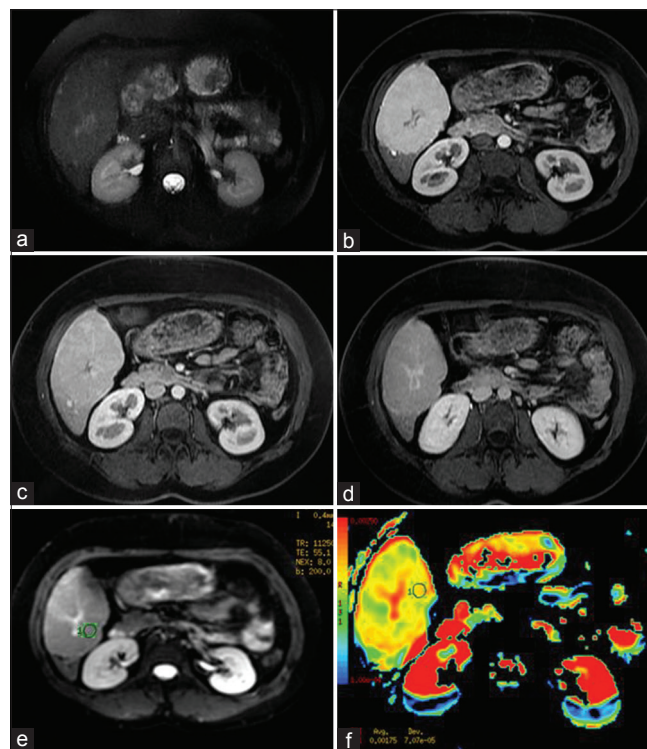


Figure 4: Focal nodular hyperplasia of the right liver in a 24-year-old woman. Axial T2-weighted fast spin echo (a), T1 after gadolinium injection of in the arterial time (b), portal (c), then late (d). The diffusion magnetic resonance imaging with b-value of 600 s/mm² (e), and apparent diffusion coefficient map (f). The FNH diagnosis was established on the presence of typical magnetic resonance imaging characteristics including homogeneous lesion, sharp contours with isosignal in T1- and T2-images, with a central area of T1-hyposignal and T2-hypersignal, the late contrast enhancement (c) and latest enhancement in the central scar was demonstrated. The apparent diffusion coefficient value in the lesion was $1.5 \times 10^{-3} \text{mm}^2/\text{s}$, whereas the apparent diffusion coefficient in the liver tissue was $2.05 \times 10^{-3} \text{mm}^2/\text{s}$

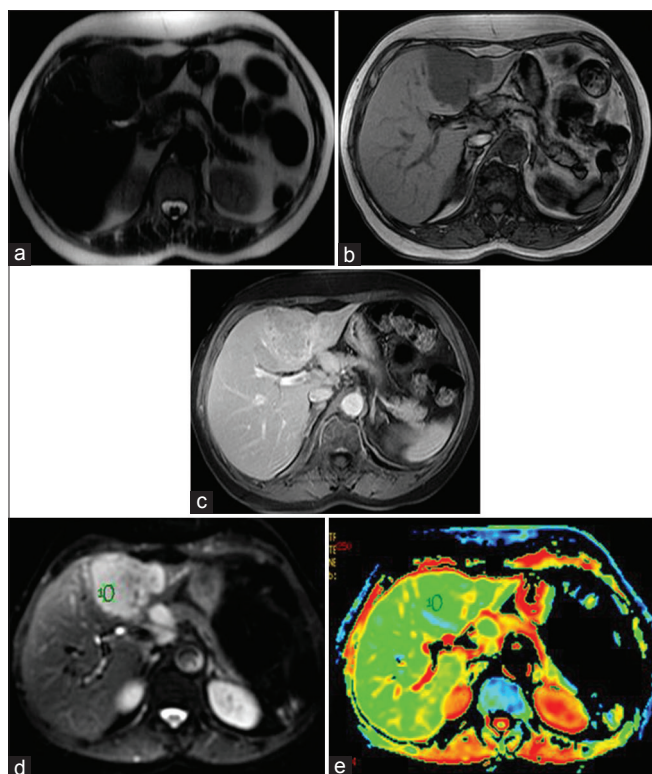


Figure 5: The left liver cholangiocarcinoma in a 56-year-old woman. The axial T2 fast spin echo (a), T1 before contrast injection (b), T1 after injection of gadolinium in portal time (c). The diffusion magnetic resonance imaging with a b-value of 600 s/mm^2 (d) and the apparent diffusion coefficient map (e). The lesion demonstrated a discrete T2-hypersignal and T1-hyposignal with discrete heterogeneous contrast enhancement. The final diagnosis of intrahepatic cholangiocarcinoma was achieved after left hepatectomy. The apparent diffusion coefficient value in the lesion was $1.15 \times 10^{-3} \text{ mm}^2/\text{s}$, whereas the liver apparent diffusion coefficient was $1.1 \times 10^{-3} \text{ mm}^2/\text{s}$

et al. demonstrated that the dMRI sensitivity and specificity are 63.5% and 86.4%, respectively, in the diagnosis of malignant tumor when using the threshold of $1.6 \times 10^{-3} \text{ mm}^2/\text{s}$ suggested by Parikh *et al.*^[15,16]

In our study, the average ADC value in the malignant lesions of $1.19 \pm 0.33 \times 10^{-3} \text{ mm}^2/\text{s}$ is significantly lower compared to benign lesions demonstrating an average ADC value of $2.26 \pm 0.75 \times 10^{-3} \text{ mm}^2/\text{s}$; these results are compliant with the literature data.^[5-7,10-11] The average ADC values in malignant lesions are variable; the lowest value ($1.04 \times 10^{-3} \text{ mm}^2/\text{s}$) is reported by Gourtsoyianni *et al.* in a study which included 13 metastases and only 2 HCC. The highest threshold ADC value was $1.52 \times 10^{-3} \text{ mm}^2/\text{s}$ was reported by Miller *et al.* that included a multicentric study of 112 HCC and 107 metastases.^[15]

Our results showed an important dispersal of the lowest ADC values of $0.33 \times 10^{-3} \text{ mm}^2/\text{s}$ in a case of lymphoma, whereas the highest ADC values of $1.88 \times 10^{-3} \text{ mm}^2/\text{s}$ in metastasis of rectal cancer. The first value is explained by hypercellular character of the lymphoma originating

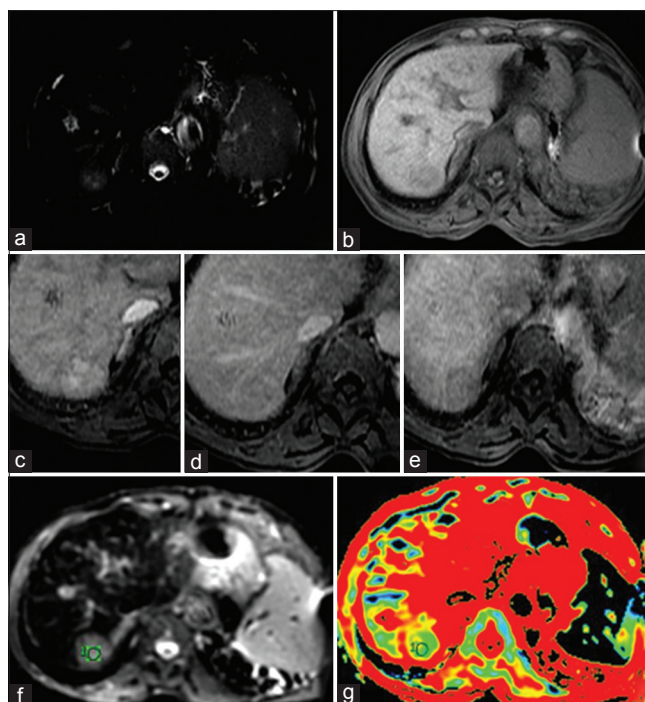


Figure 6: Hepatocellular carcinoma on cirrhosis viral C hepatitis in a 60-year-old. The axial fast spin echo T2 (a), T1 before gadolinium injection (b), T1 after the gadolinium injection in the arterial time (c), portal (d), then later (e). The diffusion magnetic resonance imaging with b-value of 600 s/mm^2 (f); the apparent diffusion coefficient maps (g). The lesion in the segment VII of the liver showed a discrete hypersignal in T2 and hyposignal in T1 with early contrast enhancement in the arterial time (c). The final hepatocellular carcinoma diagnosis was well demonstrated after surgical resection. The measured apparent diffusion coefficient in the lesion was $1.21 \times 10^{-3} \text{ mm}^2/\text{s}$, whereas the liver apparent diffusion coefficient was $1.30 \times 10^{-3} \text{ mm}^2/\text{s}$

diffusion restriction and restricted ADC. The second value is explained by the fibrous character of secondary lesion of colorectal origin.^[14-19]

In our series, the HCC and the metastases demonstrated lower average ADC values of $1.4 \pm 0.18 \times 10^{-3} \text{ mm}^2/\text{s}$ and $1.39 \pm 0.30 \times 10^{-3} \text{ mm}^2/\text{s}$, respectively, whereas Bruegel *et al.* and Gourtsoyianni *et al.* reported ADC values of $1.05 \times 10^{-3} \text{ mm}^2/\text{s}$ and $1.38 \times 10^{-3} \text{ mm}^2/\text{s}$.^[14] The metastases ADC values were between $0.94 \times 10^{-3} \text{ mm}^2/\text{s}$ and $1.50 \times 10^{-3} \text{ mm}^2/\text{s}$ and were reported by Taouli *et al.* and Parikh *et al.*, respectively.^[16,20] Our results are thus completely consistent with published literature results. The difference between the average ADC value in the HCC and the metastases is not significant in our study as well as in the literature data.^[16-21]

Thus, it is impossible to use the ADC as a single criterion to distinguish malignant and benign types of lesions. Indeed, our results confirmed the interest and usefulness of dMRI and ADC in the characterization of the hepatic lesions despite the variability of the ADC values suggested in the literature.^[16-21]

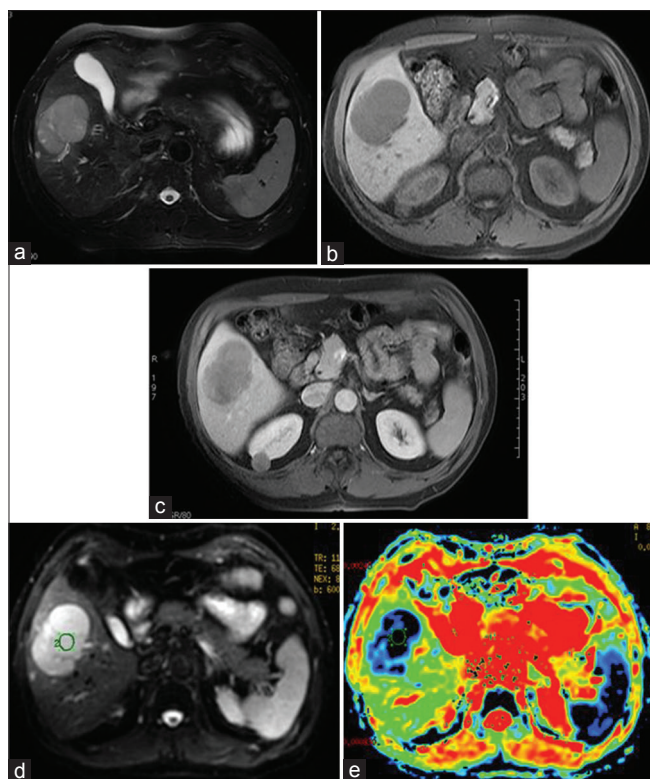


Figure 7: Lymphoma with hepatic localization in a 59-year-old man, followed for a retroviral infection. The axial T2-weighted fast spin echo (a), T1-weighted before contrast agent injection (b), T1 after gadolinium injection (c), the diffusion magnetic resonance imaging with b-value of 600 s/mm² (d), and the apparent diffusion coefficient map (e) showed a well-delineated lesion with clear hypersignal in the diffusion image and in the T2-weighted images, whereas the T1-weighted images demonstrated an hyposignal with lower enhancement after gadolinium enhancement. The diagnosis of lymphoma was established on the hepatic biopsy. The apparent diffusion coefficient in the hepatic lesion was $0.8 \times 10^{-3} \text{ mm}^2/\text{s}$, whereas the apparent diffusion coefficient in the liver was $1.6 \times 10^{-3} \text{ mm}^2/\text{s}$

CONCLUSION

The impact of the dMRI seems to be promising in the diagnostic strategy; however, it is still in the evaluation stage. Nevertheless, it should be included in the routine hepatic imaging protocols. The results of our study and the routine practice confirmed the utility of the dMRI, and particularly the ADC measurement in the characterization of the FHLs with the differentiating benign and malignant lesions.

Nevertheless, the ADC values are demonstrated to be very relative within the same category of lesions; hence, it is restricting the characterization of the solid FHLs.

Although a significant difference was revealed between benign and solid malignant lesion, the ADC values were dispersed and difficult to point the practical threshold ADC value.

Finally, the dMRI and the ADC measurements should not be considered as unique assessment criteria of the FHLs. Other MRI protocols and histological findings should be useful in

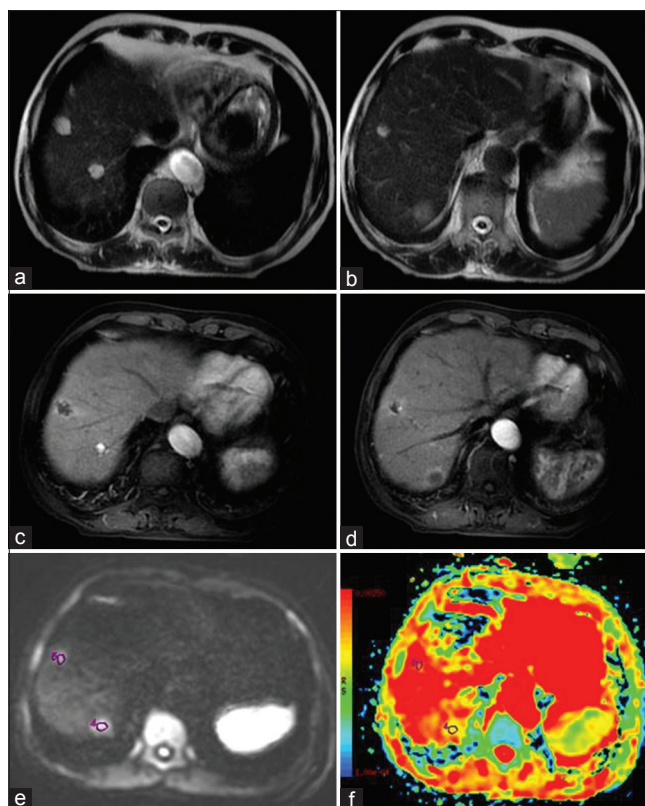


Figure 8: Association angiomas and metastasis in a 67-year-old man followed for a rectum cancer. The axial T2-weighted fast spin echo (a and b) showed recent hepatic lesion, T1 after gadolinium injection (c and d), diffusion magnetic resonance imaging with b-value of 600 s/mm² (e), and apparent diffusion coefficient maps (f) demonstrating well-limited lesions, a lesion of the segment VII of which 2 at the level of the segment VIII in frank hypersignal T2 and diffusion area in the lesion that have presented enhanced peripheral signal in the magnetic resonance imaging bolus injection images and discrete hypersignal in T2-weighted images. The apparent diffusion coefficient in the metastatic lesion was found to be $1.88 \times 10^{-3} \text{ mm}^2/\text{s}$, whereas the apparent diffusion coefficient of the liver was $1.66 \times 10^{-3} \text{ mm}^2/\text{s}$

this regards. Larger multicentric studies with standardized protocol might help in improving the determinacy of the dMRI in the FHLs.

Financial support and sponsorship

Nil.

Conflicts of interest

There are no conflicts of interest.

REFERENCES

- Housni A, Boujraf S. Multimodal magnetic resonance imaging in the diagnosis and therapeutical follow-up of brain tumors. *Neurosciences (Riyadh)* 2013;18:3-10.
- Boujraf S, Luypaert R, Shabana W, De Meirleir L, Sourbron S, Osteaux M. Study of pediatric brain development using magnetic resonance imaging of anisotropic diffusion. *Magn Reson Imaging* 2002;20:327-36.

3. Boujraf S, Luypaert R, Eisendrath H, Osteaux M. Echo planar magnetic resonance imaging of anisotropic diffusion in asparagus stems. *MAGMA* 2001;13:82-90.
4. Luypaert R, Boujraf S, Sourbron S, Osteaux M. Diffusion and perfusion MRI: Basic physics. *Eur J Radiol* 2001;38:19-27.
5. Boujraf S. Strategies for assessing diffusion anisotropy on the basis of magnetic resonance images: Comparison of systematic errors. *J Med Signals Sens* 2014;4:85-93.
6. Housni A, Boujraf S, Maaroufi M, Benzagmout M, Ezzaher K, Tizniti S. Diagnosis and monitoring of the intraparenchymal brain tumors by magnetic resonance imaging. *Med Nucl* 2014;38:469-77.
7. Taouli B, Koh DM. Diffusion-weighted MR imaging of the liver. *Radiology* 2010;254:47-66.
8. Sadowski EA, Bennett LK, Chan MR, Wentland AL, Garrett AL, Garrett RW, *et al.* Nephrogenic systemic fibrosis: Risk factors and incidence estimation. *Radiology* 2007;243:148-57.
9. Thomsen HS, Marckmann P, Logager VB. Update on nephrogenic systemic fibrosis. *Magn Reson Imaging Clin N Am* 2008;16:551-60.
10. Müller MF, Prasad P, Siewert B, Nissenbaum MA, Raptopoulos V, Edelman RR. Abdominal diffusion mapping with use of a whole-body echo-planar system. *Radiology* 1994;190:475-8.
11. Nasu K, Kuroki Y, Fujii H, Minami M. Hepatic pseudo-anisotropy: A specific artifact in hepatic diffusion-weighted images obtained with respiratory triggering. *MAGMA* 2007;20:205-11.
12. Kandpal H, Sharma R, Madhusudhan KS, Kapoor KS. Respiratory-triggered versus breath-hold diffusion-weighted MRI of liver lesions: Comparison of image quality and apparent diffusion coefficient values. *AJR Am J Roentgenol* 2009;192:915-22.
13. Taouli B, Sandberg A, Stemmer A, Parikh T, Wong S, Xu J, *et al.* Diffusion-weighted imaging of the liver: Comparison of navigator triggered and breathhold acquisitions. *J Magn Reson Imaging* 2009;30:561-8.
14. Gourtsoyianni S, Papanikolaou N, Yarmenitis S, Maris T, Karantanis A, Gourtsoyiannis N, *et al.* Intravoxel incoherent motion perfusion MR imaging: A wake-up call. *Radiology* 2008;249:748-52.
15. Miller FH, Hammond N, Siddiqi AJ, Shroff S, Khatri G, Wang Y, *et al.* Utility of diffusion-weighted MRI in distinguishing benign and malignant hepatic lesions. *J Magn Reson Imaging* 2010;32:138-47.
16. Parikh T, Drew SJ, Lee VS, Wong S, Hecht EM, Babb JS, *et al.* Focal liver lesion detection and characterization with diffusion-weighted MR imaging: Comparison with standard breath-hold T2-weighted imaging. *Radiology* 2008;246:812-22.
17. Bruegel M, Holzapfel K, Gaa J, Woertler K, Waldt S, Kiefer B, *et al.* Characterization of focal liver lesions by ADC measurements using a respiratory triggered diffusion-weighted single-shot echo-planar MR imaging technique. *Eur Radiol* 2008;18:477-85.
18. Yamada I, Aung W, Himeno Y, Nakagawa T, Shibuya H. Diffusion coefficients in abdominal organs and hepatic lesions: Evaluation with intravoxel incoherent motion echo-planar MR imaging. *Radiology* 1999;210:617-23.
19. Taouli B, Vilgrain V, Dumont E, Daire JL, Fan B, Menu Y. Evaluation of liver diffusion isotropy and characterization of focal hepatic lesions with two single-shot echo-planar MR imaging sequences: Prospective study in 66 patients. *Radiology* 2003;226:71-8.
20. Galea N, Cantisani V, Taouli B. Liver lesion detection and characterization: Role of diffusion-weighted imaging. *J Magn Reson Imaging* 2013;37:1260-76.
21. Kilickesmez O, Bayramoglu S, Inci E, Cimilli T. Value of apparent diffusion coefficient measurement for discrimination of focal benign and malignant hepatic masses. *J Med Imaging Radiat Oncol* 2009;53:50-5.